Daniel Schulze, Maurice Klopfleisch, Helmar Görls and Matthias Westerhausen*

BOX A-type monopyrrolic heterocycles modified *via* the *Suzuki-Miyaura* cross-coupling reaction

https://doi.org/10.1515/znb-2019-0125
Received August 8, 2019; accepted October 10, 2019

Abstract: The *in vivo* oxidation of heme yields bilirubin which is further degraded to the bilirubin oxidation end products (BOXes) that are biologically highly active. To study the mode of action and fate of (*Z*)-2-(4-methyl-5-oxo-3-vinyl-1,5-dihydro-2*H*-pyrrol-2-ylidene)acetamide (BOX A), the *Suzuki-Miyaura* cross-coupling reaction allows to introduce various alkenyl- and aryl-substituents in 3-position of the (*Z*)-2-(4-methyl-5-oxo-1,5-dihydro-2*H*-pyrrol-2-ylidene)acetamides (BOX A-type monopyrroles). The influence of these groups on structural and NMR-spectroscopic parameters of the central monopyrrolic system is negligible. Special focus has been given to derivatives with 3-positioned aryl substituents carrying trifluoromethyl groups for future *in vivo* ^{19}F NMR studies.

Keywords: BOXes; cross-coupling; heme degradation; pyrroles; *Suzuki-Miyaura* cross-coupling.

Dedicated to: Professor Arndt Simon on the occasion of his 80th birthday.

1 Introduction

In vivo oxidative heme degradation is catalyzed by heme oxygenases or by reactive oxygen species (ROS) leading to a stepwise degradation *via* bilirubin and biliverdin. These metabolites are further oxidatively degraded to dipyrrolic propentdyopent-type species (PDPs) and finally to the monopyrrolic birubin oxidation end products (BOXes) [1–5]. The concentration of the BOXes in human bile depends on the structure and is very low (0.1 μM for BOX C and 0.5 μM for BOXes A and B, Scheme 1) [6, 7]. The presence of an isomer of BOX C (BOX D: R^1 = Me, R^2 = CH_2CH_2COOH) has not been detected yet in human bile. The interest in these degradation end products arises from their biological activity, especially a long-lasting narrowing of cerebral blood vessels, and the assumption that these compounds play a significant role in subarachnoid hemorrhage which is responsible for 5% of all strokes with high morbidity and mortality [8].

Due to the very low concentrations it is extremely challenging to isolate these BOXes from biological or medicinal tissues and to elucidate fate and mode of action of these derivatives *in vivo*. The oxidative *in vitro* degradation of bilirubin with hydrogen peroxide in highly alkaline solution yields BOXes A [9], B [9] and C [10] with extremely poor yields allowing characterization of these derivatives but impeding studies with respect to biological activity and fate. Therefore we developed strategies for the total syntheses of these BOXes A [11], B [12], C and D [13] to elucidate their effects on biological tissues [7, 9, 14–16]. Here we report our investigation on the *Suzuki-Miyaura* cross-coupling reaction to modify the substitution pattern of BOX A-type derivatives for labeling and future investigations on the influence of certain substituents on biological activity. The *Suzuki-Miyaura* cross-coupling is a well-studied reaction to catalytically form C–C bonds in diverse compounds ranging from organic to pharmaceutical and biochemical molecules and applications [17–24].

2 Results and discussion

2.1 Synthesis of BOX A

The total synthesis of BOX A is a multi-step procedure involving the synthesis of methyl (*Z*)-2-(3-bromo-4-methyl-5-oxofuran-2(5*H*)-ylidene)acetate (**1**) [11]. During conversion of **1** to methyl (*Z*)-2-(3-bromo-4-methyl-5-oxo-1,5-dihydro-2*H*-pyrrol-2-ylidene)acetate (**3**) *via* reaction with ammonium acetate in glacial acetic acid, intermediately formed and hitherto unknown methyl 2-(3-bromo-2-hydroxy-4-methyl-5-oxo-2,5-dihydro-1*H*-pyrrol-2-yl) acetate (**2**) could be isolated (Scheme 2). In order to avoid mixtures of **2** and **3**, prolonged reaction time of 6 h and

***Corresponding author: Matthias Westerhausen,** Friedrich Schiller University Jena, Chair of Inorganic Chemistry 1, Humboldtstraße 8, D-07743 Jena, Germany, Fax: +49 (0) 3641-9-48132, E-mail: m.we@uni-jena.de
Daniel Schulze and Helmar Görls: Friedrich Schiller University Jena, Chair of Inorganic Chemistry 1, Humboldtstraße 8, D-07743 Jena, Germany
Maurice Klopfleisch: Otto von Guericke University, Medicinal Faculty, Clinic for Radiology and Nuclear Medicine, D-39120 Magdeburg, Germany

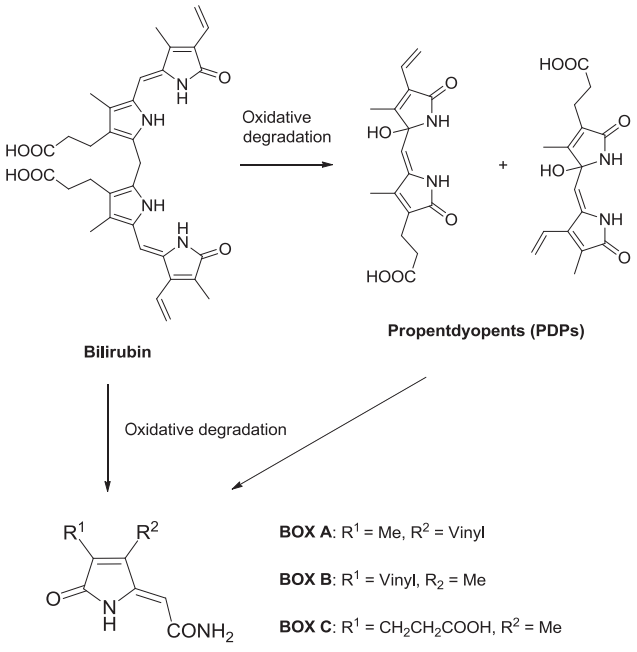

Scheme 1: The bilirubin degradation end products (BOXes A, B, C, and D) are metabolites of the oxidative degradation of heme *via* bilirubin and propentdyopents. Only BOXes A, B, and C have been detected in human bile up to now.

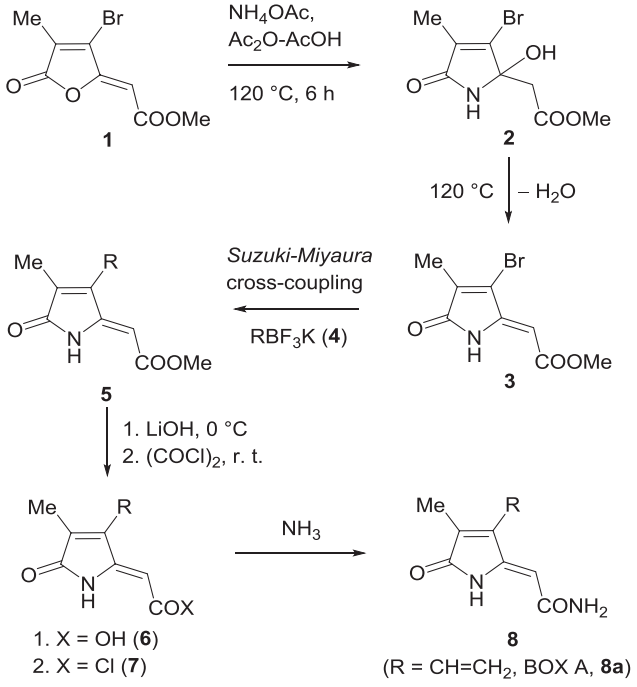

Scheme 2: The reaction sequence for the total synthesis of BOX A-type compounds **8**. BOX A (R=CH=CH_2, **8a**) is a metabolite of the oxidative degradation of bilirubin.

a temperature of 120°C were mandatory to quantitatively convert **1** to **3** without the necessity to isolate intermediate **2**. The *Suzuki-Miyaura* cross-coupling reaction proved to be a suitable method to substitute the bromo functionality of **3** with potassium vinyl-trifluoroborate (**4a**) by a vinyl group yielding methyl (*Z*)-2-(4-methyl-5-oxo-3-vinyl-1,5-dihydro-2*H*-pyrrol-2-ylidene)acetate (R=CH=CH_2, **5a**). Here we studied the scope of the *Suzuki-Miyaura* cross-coupling reaction to also attach aromatic hydrocarbyl groups or propenyl substituents. Thereafter, conversion of the ester functionality into an carboxylic amide *via* the carboxylic acid (**6a**) and the corresponding acid chloride (**7a**) yielded (*Z*)-2-(4-methyl-5-oxo-3-vinyl-1,5-dihydro-2*H*-pyrrol-2-ylidene)acetamide (BOX A, R=CH=CH_2, **8a**). This reaction sequence is depicted in Scheme 2.

The molecular structure and atom labeling scheme of methyl 2-(3-bromo-2-hydroxy-4-methyl-5-oxo-2,5-dihydro-1*H*-pyrrol-2-yl)acetate (**2**) are depicted in Fig. 1. Due to a centric space group the crystalline phase consists of a racemate of this chiral compound. Within the five-membered heterocycle significantly different C–C bond lengths are observed, excluding effective charge delocalization between the carbonyl fragment C5–O51 and the C3=C4 double bond. The N1–C2 bond is more than 10 pm longer than the N1–C5 bond. This elongation is a consequence of sp^3 hybridization of C2 and a rather crowded environment of this quaternary carbon atom. Therefore it is not astonishing that the C2–C3 and C2–C21 bond lengths are larger than the C4–C5 and C4–C41 single bonds.

In the crystalline state methyl 2-(3-bromo-2-hydroxy-4-methyl-5-oxo-2,5-dihydro-1*H*-pyrrol-2-yl)acetate (**2**) aggregates *via* intermolecular N1–H1···O23′ hydrogen bonds to the ester carbonyl moieties of the neighboring molecule (–*x*, *y*, –*z* + 0.5). Furthermore, the hydroxyl group forms an O26–H26···O51′ hydrogen bond to the carbonyl group of the nearby oxopyrrole fragment (–*x*, –*y*, –*z*). Both hydrogen bonds are nearly linear with N1–H1···O23′ and O26–H26···O51′ bond angles of 170(2)° and 172(3)° and N1···O23′ and O26···O51′ distances of 295.81(17) and 275.58(16) pm, respectively. This hydrogen bonding network leads to the formation of a strand structure in the solid state (Fig. 1, bottom).

2.2 *Suzuki-Miyaura* cross-coupling

The *Suzuki-Miyaura* cross-coupling step offers the opportunity to introduce groups other than the vinyl moiety. This alteration allows to bind substituents with functionalities that allow tracking of these monopyrrolic compounds in living organisms (such as $^{19}F\{^1H\}$ NMR spectroscopic experiments). Therefore we studied the scope of this C–C bond forming reaction between sp^2-hybridized carbon atoms that in

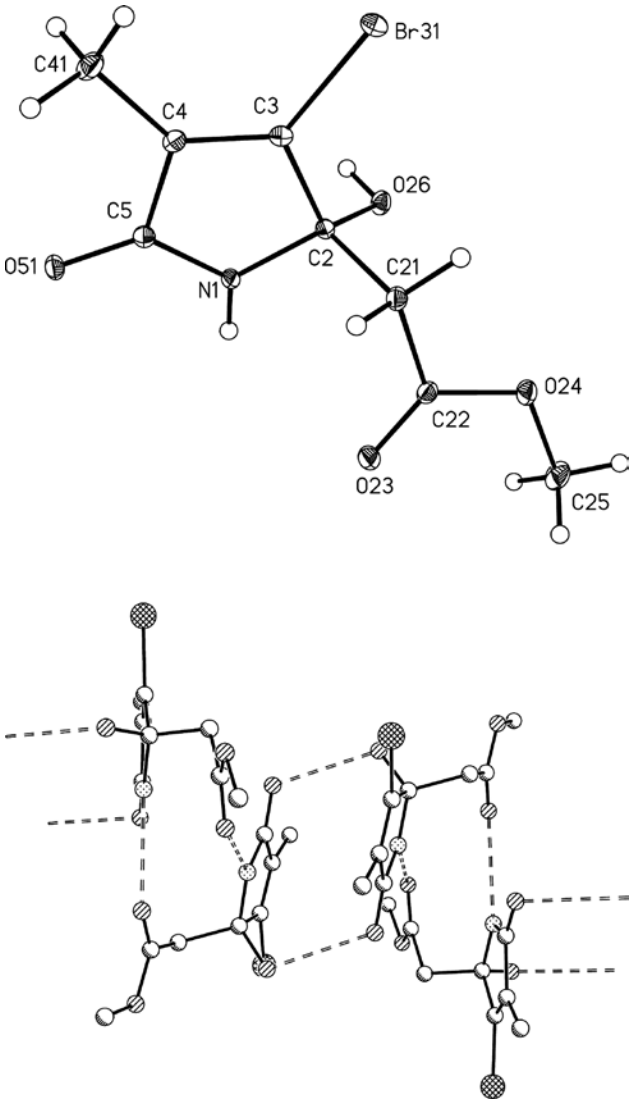

Fig. 1: Molecular structure and atom labeling scheme of methyl 2-(3-bromo-2-hydroxy-4-methyl-5-oxo-2,5-dihydro-1*H*-pyrrol-2-yl) acetate (**2**, top). The ellipsoids represent a probability of 30%. Hydrogen atoms are shown with arbitrary radii. Selected bond lengths (pm): N1–C5 135.0(2), C4–C5 149.3(2), C3–C4 133.2(2), C2–C3 152.3(2), N1–C2 145.8(2), N1–H1 83(2), C5–O51 123.5(2), C4–C41 148.3(2), C3–Br31 186.54(16), C2–O26 139.8(2), O26–H26 82(3), C2–C21 153.9(2), C21–C22 150.5(2), C22–O23 120.8(2), C22–O24 133.5(2), O24–C25 145.0(2). At the bottom, aggregation *via* hydrogen bonds is depicted. The atoms are shown with arbitrary radii, hydrogen atoms are omitted for clarity reasons.

general gave excellent isolated yields above 80%. In a typical procedure, methyl (*Z*)-2-(3-bromo-4-methyl-5-oxo-1,5-dihydro-2*H*-pyrrol-2-ylidene)acetate (**3**) and 1.5 equivalents of the corresponding potassium aryl- or alkenyl-trifluoroborate (**4b**–**4k**, 1.5 mmol, 1.5 equiv.) were dissolved in a solvent mixture of tetrahydrofuran and water (ratio 4:1) in the presence of 5 mol-% of $Pd(PPh_3)_2Cl_2$ and three equivalents of CsF. Then the reaction mixture was heated under reflux for 18 h in a nitrogen atmosphere. In all cases the *Z*-isomeric form was isolated because this diastereomer is stabilized *via* formation of an intramolecular N–H···O hydrogen bond between the pyrrole unit and the ester carbonyl functionality. The outcome of this screening is summarized in Table 1.

Table 1: Synthesis of 3-aryl- and 3-alkenyl-substituted methyl (*Z*)-2-(4-methyl-5-oxo-1,5-dihydro-2*H*-pyrrol-2-ylidene)acetates (**5a**–**5k**) *via Suzuki-Miyaura* cross-coupling reactions using RBF_3K (**4a**–**4k**) according to Scheme 2.

Entry	R	Product	Yield (%)	Ref.
1	$CH{=}CH_2$ (**4a**)	**5a**	84	[11]
2	(*E*)-CH=CH–CH_3 (**4b**)	**5b**	90	This work
3	$C(Me){=}CH_2$ (**4c**)	**5c**	93	This work
4	C_6H_5 (**4d**)	**5d**	90	This work
5	C_6H_4-3-CH_3 (**4e**)	**5e**	82	This work
6	C_6H_4-4-CH_3 (**4f**)	**5f**	91	This work
7	C_6H_4-4-$C(CH_3)_3$ (**4g**)	**5g**	89	This work
8	C_6H_4-4-CF_3 (**4h**)	**5h**	94	This work
9	C_6H_3-3,5-$(CF_3)_2$ (**4i**)	**5i**	98	This work
10	2-naphthyl (**4j**)	**5j**	85	This work
11	2-furanyl (**4k**)	**5k**	82	This work

Due to the fact that ^{19}F-labeled BOX A derivatives attracted our special interest, the molecular structure and the atom labeling scheme of methyl (*Z*)-2-(4-methyl-5-oxo-3-(4-trifluoromethylphenyl)-1,5-dihydro-2*H*-pyrrol-2-ylidene)acetate (**5h**) are depicted in Fig. 2. The molecular representations of the derivatives **5b**–**5g** and **5j** are shown in the Supporting Information (available online) verifying that exclusively *Z*-isomeric congeners were isolated and crystallized.

For comparison reasons selected structural parameters of 3-alkenyl- (entries 2 and 3) and 3-aryl-substituted (entries 4–9) methyl (*Z*)-2-(4-methyl-5-oxo-1,5-dihydro-2*H*-pyrrol-2-ylidene)acetates **5** are listed in Table 2. The numbering of the carbon atoms obeys to the IUPAC recommendation as used for the atom denominations in these compounds. The bond lengths of all compounds deviate in a very narrow range with the phenyl (entry 4, **5d**) and naphthyl derivatives (entry 9, **5j**) showing the shortest C3=C4 double bonds and the longest C3–C31 and N1–C5 bonds. However, these differences are very small and in the order of the estimated standard deviations. In summary, the substituents in 3-position show a negligible influence on the structural parameters of the 3-alkenyl- (entries 2 and 3) and 3-aryl-substituted (entries 4–9) methyl (*Z*)-2-(4-methyl-5-oxo-1,5-dihydro-2*H*-pyrrol-2-ylidene)acetates.

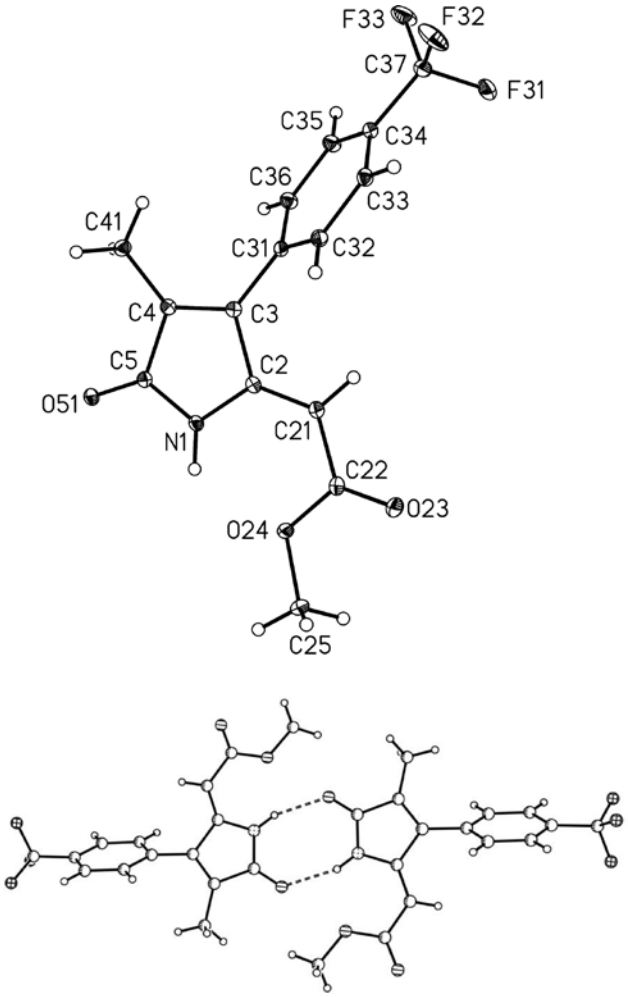

Fig. 2: Molecular structure and atom labeling scheme of methyl (*Z*)-2-(4-methyl-5-oxo-3-(4-trifluoromethyl)-1,5-dihydro-2*H*-pyrrol-2-ylidene)acetate (**5h**, top). The ellipsoids represent a probability of 30%, hydrogen atoms are drawn with arbitrary radii. Selected bond lengths (pm) are listed in Table 2. At the bottom, dimerization *via* intermolecular hydrogen bonds is depicted. All atoms are shown with arbitrary radii.

The 3-alkenyl- (entries 1 and 2, Table 3) and 3-aryl-substituted (entries 3–8) methyl (*Z*)-2-(4-methyl-5-oxo-1,5-dihydro-2*H*-pyrrol-2-ylidene)acetates **5** form dimers in the crystalline state due to aggregation *via* intermolecular N1–H1···O51′ hydrogen bonds (Table 3). These highly asymmetric hydrogen bonds are rather weak and the intermolecular N1···O51′ distances adopt values between 290 and 320 pm. The N–H stretching vibrations show values around 3300 cm^{-1} supporting the weak nature of these hydrogen bonds. The N1–H1···O51′ bond angles adopt rather large values between 145° and 165°. At the bottom of Fig. 2, dimerization *via* intermolecular hydrogen bonds is depicted.

2.3 Syntheses and molecular structures of BOX A-derived congeners

As outlined above, we were especially interested in the ^{19}F labeled congeners for future studies on degradation and fate of the monopyrrolic compounds in biological systems. Therefore, we converted the ester functionalities of **5h** and **5i** with LiOH at $T = 0°C$ into the corresponding carboxylic acids yielding (*Z*)-2-(4-methyl-5-oxo-3-(4-trifluoromethylphenyl)-1,5-dihydro-2*H*-pyrrol-2-ylidene)acetic acid (**6h**) and (*Z*)-2-(4-methyl-5-oxo-3-(3,5-bis(trifluoromethyl)phenyl)-1,5-dihydro-2*H*-pyrrol-2-ylidene)acetic acid (**6i**), respectively. An additional purification was not necessary, but the purity was then sufficient for the subsequent derivatization protocol. The reaction of these acids with oxalyl chloride at room temperature yielded the corresponding acetyl chlorides, (*Z*)-2-(4-methyl-5-oxo-3-(4-trifluoromethylphenyl)-1,5-dihydro-2*H*-pyrrol-2-ylidene)acetyl chloride (**7h**) and (*Z*)-2-(4-methyl-5-oxo-3-(3,5-bis(trifluoromethyl)phenyl)-1,5-dihydro-2*H*-pyrrol-2-ylidene)acetyl chloride (**7i**) as depicted in Scheme 2. Finally, these compounds were dissolved in THF and ammonia was added at $T = 0°C$. Then the reaction mixture was warmed to room temperature. Contrary to the yields of **6** and **7** which were excellent, the final step proceeded with yields of only 67% and 53% for (*Z*)-2-(4-methyl-5-oxo-3-(4-trifluoromethylphenyl)-1,5-dihydro-2*H*-pyrrol-2-ylidene)acetamide (**8h**) and (*Z*)-2-(4-methyl-5-oxo-3-(3,5-bis(trifluoromethyl)phenyl)-1,5-dihydro-2*H*-pyrrol-2-ylidene)acetamide (**8i**).

The molecular structures and atom labeling schemes of **8h** and **8i** are depicted in Figs. 3 and 4. The crystal structure of **8h** contains two crystallographically independent molecules A and B with very similar structural parameters and an additional methanol molecule which is involved in an extended hydrogen bonding network.

Selected bond lengths of BOX A (**8a**) [11], **8h** (molecules **A** and **B**), and **8i** are compared in Table 4. The structural parameters of the pyrrole ring are very similar and the transformation of the ester functionality into an amide does not affect the endocyclic N–C and C–C bond lengths. The exocyclic aryl groups at C3 are orientated nearly perpendicular to the pyrrole ring prohibiting significant interactions between these π systems. Hence, typical C3–C31 single bonds are observed which are comparable to the C4–C41 bond lengths to the methyl substituents. The amide functionality shows a slight charge delocalization within the O23–C22–N23 unit, leading to larger C22–O23 bond lengths compared to C5–O51 and shorter C22–N23 bonds in comparison to the endocyclic N1–C2/5 bond lengths.

Table 2: Selected bond lengths (pm) of 3-alkenyl- (entries 2 and 3) and 3-aryl-substituted (entries 4–9) methyl (*Z*)-2-(4-methyl-5-oxo-1,5-dihydro-2*H*-pyrrol-2-ylidene)acetates (**5a**–**5j**).

Entry	Comp.	N1–C2	C2–C3	C3=C4	C4–C5	N1–C5	C2=C21	C3–C31	C5=O51	N1–H1	Ref.
1	**2**	145.8(2)	152.3(2)	133.2(2)	149.3(2)	135.0(2)	153.9(2)	186.54(16)[c]	123.5(2)	83(2)	This work
2	**5b**	138.9(2)	149.2(2)	135.8(2)	148.1(2)	137.4(2)	134.6(2)	145.6(2)	122.6(2)	91(2)	This work
3	**5c A**[a]	138.0(2)	148.5(2)	133.9(2)	149.1(2)	138.8(2)	134.5(2)	148.2(2)	121.6(2)	86(2)	This work
	5c B[a]	138.4(2)	148.0(2)	134.3(2)	149.2(2)	137.7(2)	134.5(2)	148.7(2)	121.6(2)	86(2)	
4	**5d A**[a]	138.1(2)	148.1(2)	134.6(2)	149.1(2)	137.8(2)	134.7(2)	147.8(2)	122.1(2)	90(2)	This work
	5d B[a]	138.4(2)	148.5(2)	134.6(2)	148.5(2)	138.0(2)	134.7(2)	147.6(2)	122.1(2)	88(2)	
5	**5e A**[a]	138.6(2)	148.5(2)	135.1(2)	148.4(2)	137.5(2)	134.5(2)	147.8(2)	122.6(2)	87(2)	This work
	5e B[a]	138.2(2)	148.3(2)	135.2(2)	148.7(2)	137.6(2)	134.2(2)	147.6(2)	122.3(2)	84(2)	
6	**5f A**[b]	138.1(3)	148.8(3)	134.2(4)	148.9(3)	138.1(3)	134.6(4)	148.3(3)	122.0(3)	85(3)	This work
	5f B[b]	139.1(3)	148.5(3)	135.0(3)	148.8(3)	137.8(3)	134.6(4)	148.0(3)	122.0(3)	90(3)	
	5f C[b]	138.6(3)	148.3(3)	134.8(3)	148.9(3)	137.3(3)	134.8(3)	147.6(3)	122.5(3)	86(3)	
	5f D[b]	139.0(3)	148.5(3)	134.3(3)	149.0(3)	137.4(3)	134.6(3)	147.6(3)	122.5(3)	86(3)	
7	**5g**	138.7(2)	148.1(2)	134.6(2)	149.5(2)	137.9(2)	134.2(2)	148.4(2)	121.9(2)	88(2)	This work
8	**5h**	139.3(2)	148.5(2)	135.2(2)	148.7(2)	137.5(2)	134.9(2)	147.6(2)	122.3(2)	89(2)	This work
9	**5j**	139.1(2)	148.1(2)	134.5(2)	148.5(2)	137.8(2)	135.0(2)	147.6(2)	122.2(2)	89(2)	This work

For comparison, compound **2** (entry 1) is included. [a]The asymmetric unit contains two molecules A and B. [b]The asymmetric unit contains four molecules A, B, C, and D. [c]C3–Br31 bond length.

Table 3: Selected bond lengths (pm) and angles (deg.) of the intermolecular hydrogen bonds of 3-alkenyl- (entries 1 and 2) and 3-aryl-substituted (entries 3–8) methyl (*Z*)-2-(4-methyl-5-oxo-1,5-dihydro-2*H*-pyrrol-2-ylidene)acetates (**5a**–**5j**).

Entry	Comp.	N1–H1	O51′···H1[c]	N1···O51′[c]	N1–H1···O51′[c]	Ref.
1	**5b**	91(2)	205(2)	292.84(16)	162(2)	This work
2	**5c A**[a]	86(2)	235(2)	312.72(19)	151(2)	This work
	5c B[a]	84(2)	243(2)	318.80(18)	151.3(19)	
3	**5d A**[a]	90(2)	211(2)	295.74(15)	158.5(16)	This work
	5d B[a]	88(2)	224(2)	305.65(15)	155.5(16)	
4	**5e A**[a]	87(2)	207(2)	289.96(19)	158.5(19)	This work
	5e B[a]	84(2)	237(2)	309.6(2)	145.1(19)	
5	**5f A**[b]	85(3)	212(4)	292.9(3)	159(3)	This work
	5f B[b]	90(3)	205(3)	293.0(3)	165(3)	
	5f C[b]	86(3)	206(3)	289.6(3)	163(3)	
	5f D[b]	86(3)	213(3)	294.6(3)	159(3)	
6	**5g**	88(2)	221(2)	302.31(18)	153(2)	This work
7	**5h**	89(2)	206(2)	290.56(18)	158(2)	This work
8	**5j**	89(2)	207(2)	291.26(19)	157(2)	This work

[a]The asymmetric unit contains two molecules A and B. [b]The asymmetric unit contains four molecules A, B, C, and D. [c]Intermolecular distances to the neighboring molecule.

Compound **8h** forms an extended hydrogen bonding network *via* intermolecular N1A–H1A···O23B (146.1(18)°, N1A···O23B 273.72(15) pm) and N1B–H1B···O51A (155.8(18)°, N1B···O51A 305.68(16) pm) bridges. In addition, the methanol molecule is connected to the amide functionalities (N23A–H23A···O1M and O1M–H1M···O23B). The other amide N23A–H23B coordinates to the amide carbonyl group of the neighboring molecule. This extended hydrogen bonding network significantly reduces the solubility of **8h** in common organic solvents. In contrast to this aggregation, compound **8i** with the bulkier 3,5-bis(trifluoromethyl)phenyl groups only forms dimers in the crystalline state but of a different nature than observed for the derivative **5**. Dimerization occurs via intermolecular hydrogen bonds between the amide functionalities (N23–H23A···O23′ 178(4)°, N23···O23′ 293.8(3) pm) whereas the N1–H1 fragment shows no short contacts to Lewis basic sites of neighboring molecules.

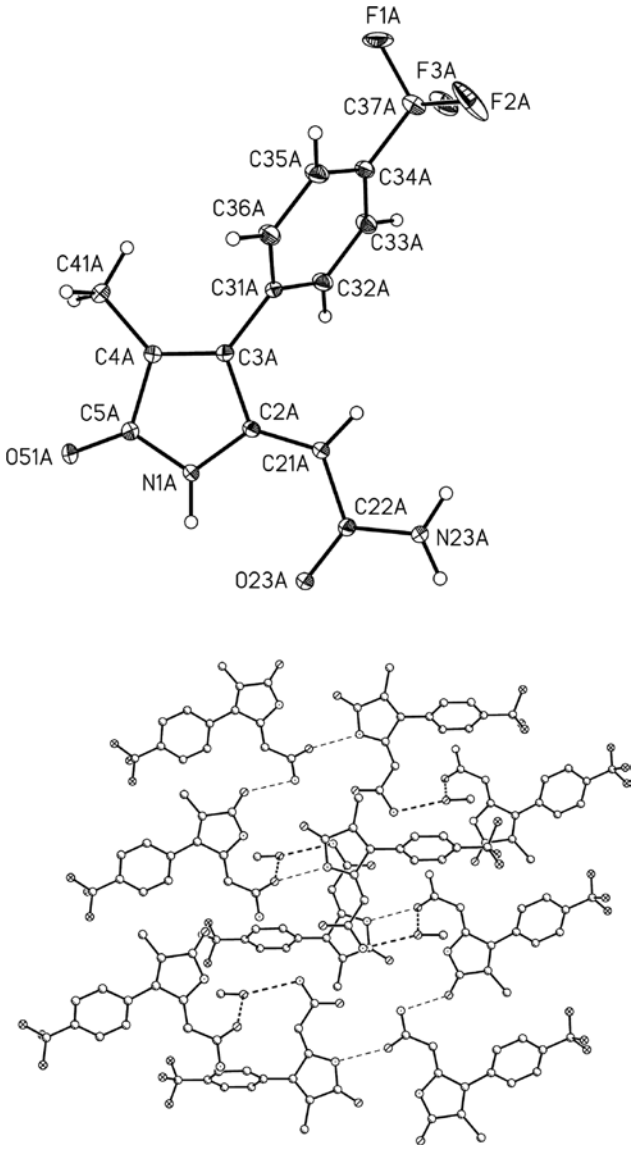

Fig. 3: Molecular structure and atom labeling scheme of (*Z*)-2-(4-methyl-5-oxo-3-(4-trifluoromethylphenyl)-1,5-dihydro-2*H*-pyrrol-2-ylidene)acetamide (**8h**, top). The ellipsoids represent a probability of 30%, hydrogen atoms are shown with arbitrary radii. At the bottom, aggregation *via* hydrogen bonds (dotted lines) is shown. Only the non-hydrogen atoms are drawn with arbitrary radii.

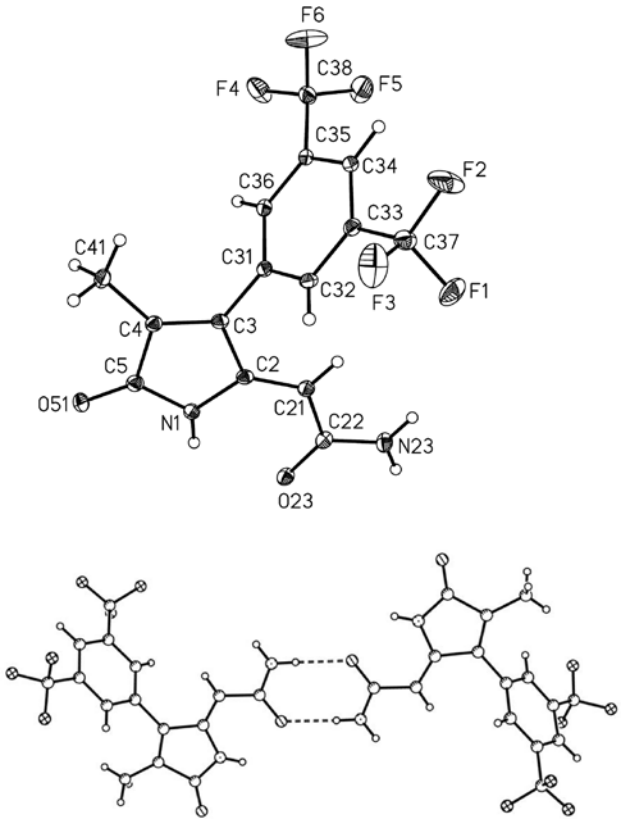

Fig. 4: Molecular structure and atom labeling scheme of (*Z*)-2-(4-methyl-5-oxo-3-(3,5-bis(trifluoromethyl)phenyl)-1,5-dihydro-2*H*-pyrrol-2-ylidene)acetamide (**8i**, top). The ellipsoids represent a probability of 30%, hydrogen atoms are shown with arbitrary radii. At the bottom, dimerization via hydrogen bonds (dotted lines) is depicted. All atoms are shown with arbitrary radii for clarity reasons.

2.4 NMR spectroscopy

The $^{13}C\{^1H\}$ NMR chemical shifts of the pyrrole units of 3-aryl- and 3-alkenyl-substituted methyl (*Z*)-2-(4-methyl-5-oxo-1,5-dihydro-2*H*-pyrrol-2-ylidene)acetates **5** as well as methyl (*Z*)-2-(4-methyl-5-oxo-1,5-dihydro-2*H*-pyrrol-2-ylidene)acetamides **8** are listed in Table 5. The atom numbering is in accordance with the IUPAC nomenclature and identical to the molecule representations in Figs. 2–4. Furthermore, the δ values of the groups at C2 and C4 are included in this table. The solubility of the methyl acetates **5** in common organic solvents is significantly higher than the solubility of the acetamides **8**. Therefore the latter compounds had to be dissolved in DMSO-d_6 in order to break down the hydrogen bonding network and to obtain reliable and meaningful $^{13}C\{^1H\}$ NMR spectra.

The $^{13}C\{^1H\}$ NMR shifts of the pyrrole carbon atoms C2 and C5, which bind to N1, vary within very narrow ranges around 171 and 149 ppm, respectively. The C3 atoms are bound to alkenyl and aryl groups and the influence of these substituents on the chemical shifts are also very small. In addition, the nature of the functional group of C22 (ester for entries 1–11, compound **5**; amide for entries 12–14, derivative **8**) shows a negligible influence on the chemical shift of this carbon atom. In agreement with the negligible influence of the substituents at C3 on the chemical shifts of the carbon atoms of the pyrrole ring, also the $\delta(^{13}C\{^1H\})$ values of the C4-bound methyl group C41 vary only within a very narrow range of 9.5 ± 0.5 ppm. However,

Table 4: Selected bond lengths (pm) of 3-aryl- and 3-alkenyl-substituted methyl (*Z*)-2-(4-methyl-5-oxo-1,5-dihydro-2*H*-pyrrol-2-ylidene) acetamides (numbering of pyrrol atoms according to IUPAC recommendation, *exo*-positioned atoms are numbered with a second digit).

	8a (BOX A)	8h (molecule A)	8h (molecule B)	8i
N1–C2	138.8(3)	138.80(17)	139.17(17)	138.4(3)
C2–C3	147.7(3)	148.28(18)	148.37(18)	147.7(3)
C3=C4	135.2(3)	134.59(19)	135.26(19)	134.5(4)
C4–C5	148.8(3)	149.51(18)	148.77(19)	149.9(3)
N1–C5	136.9(3)	137.43(18)	136.73(18)	137.9(3)
$C2{=}C21_{exo}$	133.9(3)	134.32(19)	134.77(19)	134.4(4)
$C21{-}C22_{amide}$	147.6(3)	147.84(18)	147.61(18)	147.7(3)
$C22_{amide}{-}O23$	124.9(3)	124.92(17)	124.63(17)	124.3(3)
$C22_{amide}{-}N23$	133.6(3)	133.88(18)	133.37(18)	134.2(4)
$C3{-}C31_{exo}$	147.0(3)	149.09(18)	148.02(18)	149.0(3)
$C4{-}C41_{Me}$	148.8(3)	149.34(19)	148.72(19)	148.5(4)
C5=O51	122.3(2)	122.72(17)	122.57(17)	121.6(3)
Ref.	[11]	This work	This work	This work

Table 5: $^{13}C\{^1H\}$ chemical shifts (ppm) of the pyrrole units of 3-alkenyl- (entries 1–3 and 12) and 3-aryl-substituted (entries 4–11 as well as 13 and 14) methyl (*Z*)-2-(4-methyl-5-oxo-1,5-dihydro-2*H*-pyrrol-2-ylidene)acetates **5** as well as methyl (*Z*)-2-(4-methyl-5-oxo-1,5-dihydro-2*H*-pyrrol-2-ylidene)acetamides **8** (numbering of pyrrole atoms according to IUPAC recommendation, exo-positioned atoms are numbered with a second digit; see Figs. 2–4).

Entry	Comp.	Solvent	C2	C3	C4	C5	C21	C22	C41	Ref.
1	**5a**	DMSO-d_6	149.0	138.5	131.1	171.1	94.3	166.3	9.6	[11]
2	**5b**	DMSO-d_6	149.5	139.7	129.1	171.5	93.9	166.4	9.6	This work
3	**5c**	DMSO-d_6	148.9	146.0	130.8	171.1	94.9	166.1	9.0	This work
4	**5d**	DMSO-d_6	149.6	143.8	132.2	171.1	95.9	165.9	9.2	This work
5	**5e**	DMSO-d_6	149.7	144.0	132.0	171.1	95.9	166.0	9.2	This work
6	**5f**	DMSO-d_6	149.7	143.9	131.8	171.1	95.8	166.0	9.1	This work
7	**5g**	DMSO-d_6	151.6	143.8	131.8	171.2	95.9	165.9	9.2	This work
8	**5h**	$CDCl_3$	150.0	142.8	134.6	170.7	96.5	167.6	9.6	This work
9	**5i**	$CDCl_3$	149.5	141.1	136.0	170.1	96.5	167.4	9.7	This work
10	**5j**	DMSO-d_6	149.6	143.9	132.7	171.1	96.2	166.0	9.6	This work
11	**5k**	DMSO-d_6	147.3	145.1	130.1	170.6	96.5	166.0	10.0	This work
12	**8a**	DMSO-d_6	145.7	139.1	130.8	170.3	98.5	168.0	9.3	[11]
13	**8h**	DMSO-d_6	146.0	142.1	132.7	170.0	100.3	167.7	9.1	This work
14	**8i**	DMSO-d_6	146.0	140.7	134.0	169.7	100.2	167.6	9.1	This work

the methyl resonances are high field-shifted compared to simple compounds with methyl groups bound to alkene moieties as in propene ($\delta(CH_3) = 19.4$ ppm), (*Z*)-2-butene ($\delta(CH_3) = 11.4$ ppm), (*E*)-2-butene ($\delta(CH_3) = 16.8$ ppm), (*Z*)-penta-1,3-diene ($\delta(CH_3) = 12.8$ ppm), and (*E*)-penta-1,3-diene ($\delta(CH_3) = 17.2$ ppm) [25].

3 Conclusion

During the synthesis of methyl (*Z*)-2-(3-bromo-4-methyl-5-oxo-1,5-dihydro-2*H*-pyrrol-2-ylidene)acetate (**3**) we observed the intermediate hydration product **2** which we were able to prepare with a yield of 78%. Isolation and characterization of this intermediately formed methyl 2-(3-bromo-2-hydroxy-4-methyl-5-oxo-2,5-dihydro-1*H*-pyrrol-2-yl)acetate (**2**) verifies that the ammonia molecule attacks the ring at the carbonyl group rather than at the alkylidene fragment. At higher reaction temperatures the water molecule is eliminated and the pyrrole derivative **3** is formed. Isolation of **2** prior to the conversion to **3** is not needed but higher reaction temperatures are recommended in order to avoid the formation and isolation of mixtures of **2** and **3**.

The *Suzuki-Miyaura* cross-coupling sequence allows to form C–C bonds between sp^2-hybridized carbon atoms leading to alkenyl- and aryl-substituted pyrroles. Thus the palladium-mediated reaction of methyl (*Z*)-2-(3-bromo-4-methyl-5-oxo-1,5-dihydro-2*H*-pyrrol-2-ylidene) acetate (**3**) with potassium aryl- or alkenyl-trifluoroborate (**4**) yields 3-alkenyl- or 3-aryl-substituted methyl (*Z*)-2-(4-methyl-5-oxo-1,5-dihydro-2*H*-pyrrol-2-ylidene) acetate (**5**). Generally the yields of isolated products are above 80% making this protocol a powerful procedure to exchange the bromine atom of the pyrroles **3** by alkenyl- and aryl-groups in 3-position. The influence of this substituent on structural and NMR spectroscopic parameters of the pyrrolylidene fragment is negligible. Furthermore, these groups do not hamper the conversion to the amides **8** as we could demonstrate for the synthesis of (*Z*)-2-(4-methyl-5-oxo-3-(4-trifluoromethylphenyl)-1,5-dihydro-2*H*-pyrrol-2-ylidene)acetamide (**8h**) and (*Z*)-2-(4-methyl-5-oxo-3-(3,5-bis(trifluoromethyl)phenyl)-1,5-dihydro-2*H*-pyrrol-2-ylidene)acetamide (**8i**) in analogy to the preparation of biologically highly active (*Z*)-2-(4-methyl-5-oxo-3-vinyl-1,5-dihydro-2*H*-pyrrol-2-ylidene) acetamide (BOX A, **8a**).

Contrary to the structural and NMR parameters that remain nearly unaffected by the substituents in 3-position, solubility of the acetamides **8** and methyl acetates **5** are strikingly different due to the formation of hydrogen bonding networks. The esters **5** form dimers in the solid state and are quite soluble in common organic solvents whereas the acetamide **8h** with a 4-trifluoromethylphenyl substituent is only very sparingly soluble due to fact that the amide group is involved in extended hydrogen bonding networks. Contrary to the molecular parameters like bond lengths and chemical NMR shifts, aggregation of **8** via hydrogen bonds in the solid state is highly influenced by the substituents at C31 and hence, **8i** with the bulkier 3,5-bis(trifluoromethyl)phenyl group only forms dimers *via* intermolecular hydrogen bonds between the amide functionalities. Increasingly bulky groups reduce the degree of aggregation, enhancing solubility in common organic solvents.

This derivatization *via* the *Suzuki-Miyaura* cross-coupling reaction allows to introduce ^{19}F labeled groups to follow mode of action and fate of these BOX A-type monopyrrolic heterocycles by ^{19}F NMR spectroscopy. Future *in vivo* studies must show to what extent these substituents in 3-position of the pyrrole ring influence and alter the biological activity due to their increasingly bulky groups (e.g. for key-lock-type interactions) and their different ability and degree to form intermolecular hydrogen bonding networks.

4 Experimental section

The substrates methyl (*Z*)-2-(3-bromo-4-methyl-5-oxofuran-2(5*H*)-ylidene)acetate (**1**) and methyl (*Z*)-2-(3-bromo-4-methyl-5-oxo-1,5-dihydro-2*H*-pyrrol-2-ylidene) acetate (**3**) were prepared according to literature protocols [6]. ^1H, ^{13}C and ^{19}F NMR spectra were recorded on Bruker AC250, AC400 and AC600 spectrometers using the residual solvent resonances (^1H and ^{13}C NMR) as internal standards. Chemical shifts (δ) are reported in ppm. $CDCl_3$ ($\delta(^1H) = 7.26$, $\delta(^{13}C) = 77.2$), CD_2Cl_2 ($\delta(^1H) = 5.32$, $\delta(^{13}C) = 53.8$), and DMSO-d_6 ($\delta(^1H) = 2.49$, $\delta(^{13}C) = 39.5$) were used as solvents for NMR experiments [26]. IR bands (ν) are reported in cm^{-1}. Mass spectrometric experiments were performed on Finnigan MAT SSQ 710 and ThermoFinnigan MAT 95 XL instruments. Elemental analyses were provided by the Institute of Organic Chemistry and Macromolecular Chemistry, Friedrich Schiller University Jena, using a Leco CHNS-932 Elemental Analyzer. Merck silica gel 60 (0.040–0.063 mm) was used for column chromatography. Physical data and molecular structures of the compounds **5b**–**5g** as well as **5j** and **5k** are supplied in the Supporting Information available online.

4.1 Methyl 2-(3-bromo-2-hydroxy-4-methyl-5-oxo-2,5-dihydro-1*H*-pyrrol-2-yl)acetate (2)

Method A: A solution of methyl (*Z*)-2-(3-bromo-4-methyl-5-oxofuran-2(5*H*)-ylidene)acetate (**1**) (150 mg, 0.61 mmol), ammonium acetate (234 mg, 3.04 mmol) and acetic anhydride (1 drop) in glacial acetic acid (4 mL) was stirred at 70°C for 5 h. After cooling to r. t., the solvent was evaporated to dryness and the solid residue taken up in 30 mL of ethyl acetate. The solution was washed with water (2×10 mL) and brine (10 mL) and the combined aqueous layers were extracted once with ethyl acetate (10 mL). The combined organic layers were dried over anhydrous Na_2SO_4 and the solvent removed *in vacuo*. The residue was transferred into a frit, washed with a small amount of dichloromethane and dried *in vacuo* to provide **2** as a colorless solid (yield: 125 mg, 78%).

Method B: An aqueous ammonia solution (1 mL, 25%) was added to a solution of methyl (*Z*)-2-(3-bromo-4-methyl-5-oxofuran-2(5*H*)-ylidene)acetate (**1**) (230 mg, 0.93 mmol) in 10 mL of methanol. After stirring at r. t. for 1 h the solvent was removed *in vacuo* and the remaining orange solid was taken up in water (10 mL) and extracted with ethyl acetate (3×15 mL). The combined organic layers were dried over anhydrous Na_2SO_4 and the solvents removed *in vacuo*, yielding a pale yellow solid which was

recrystallized from ethyl acetate to provide colorless needles of **2**. The crystals were collected, washed with a small amount of ethyl acetate and dried *in vacuo* (yield: 72 mg, 29%).

Physical data of **2**: ^{1}H NMR (400 MHz, $CDCl_3$, 297 K): δ = 7.03 (s, 1H, N*H*), 3.78 (s, 3H, COOCH_3), 3.43 (s, 1H, O*H*), 3.17 (d, J = 16.2 Hz, 1H, CH_AH$_B$), 2.50 (d, J = 16.2 Hz, 1H, CH$_A$$H_B$), 1.88 (s, 3H, C$H_3$). – ^{1}H NMR (400 MHz, DMSO-d_6, 297 K): δ = 8.68 (s, 1H, N*H*), 6.45 (s, 1H, O*H*), 3.54 (s, 3H, COOCH_3), 2.80 (d, J = 15.0 Hz, 1H, CH_AH$_B$), 2.76 (d, J = 15.0 Hz, 1H, CH$_A$$H_B$), 1.70 (s, 3H, C$H_3$). – ^{13}C{^{1}H} NMR (101 MHz, DMSO-d_6, 297 K): δ = 168.70 (*C*ONH), 168.29 (*C*OOCH$_3$), 139.65 (*C*–Br), 132.97 (*C*–CH$_3$), 85.82 (*C*–OH), 51.39 (COO*C*H$_3$), 41.30 (*C*H$_2$), 9.87 (*C*H$_3$). – MS (DEI): *m/z* (%) = 265 (22) [M(^{81}Br)]$^+$, 263 (20) [M(^{79}Br)]$^+$, 248 (37), 246 (36), 234 (50), 232 (52), 216 (11), 214 (13), 192 (87), 190 (94), 184 (100), 174 (27), 172 (25). – Elemental analysis ($C_8H_{10}BrNO_4$, 264.08): calcd.: C 36.39, H 3.82, N 5.30; found C 36.33, H 3.70, N 5.43.

4.2 General procedure for 3-aryl- and 3-alkenyl-substituted methyl (*Z*)-2-(4-methyl-5-oxo-1,5-dihydro-2*H*-pyrrol-2-ylidene)acetates (5b–5k)

A solution of 246 mg of methyl (*Z*)-2-(3-bromo-4-methyl-5-oxo-1,5-dihydro-2*H*-pyrrol-2-ylidene)acetate (**3**) (1 mmol), the corresponding potassium aryl- or alkenyltrifluoroborate (**4b**–**4k**, 1.5 mmol, 1.5 equiv.), 35.1 mg of $Pd(PPh_3)_2Cl_2$ (0.05 mmol, 5 mol-%) and 456 mg of CsF (3 mmol, 3 equiv.) in 10 mL of a degassed mixture of tetrahydrofuran and water (ratio 4:1) was heated under reflux for 18 h in a nitrogen atmosphere. After complete conversion and cooling to r. t. 50 mL of diethyl ether was added. The organic layer was separated, washed twice with 25 mL of water and three times with 25 mL of brine. The organic phase was dried over anhydrous sodium sulfate. Then the volatiles were removed *in vacuo* and a subsequent chromatographic purification (silica gel, petroleum ether-ethyl acetate 1:1) gave analytically pure products **5b**–**5k**.

Physical data of **5h**: Yield: 238 mg (0.76 mmol, 94%), colorless solid. – ^{1}H NMR (400.21 MHz, $CDCl_3$, 297 K): δ = 9.30 (s, br, 1H, N*H*), 7.75 (d, $^3J_{H,H}$ = 8.2 Hz, 2H, *m*-CH_{pCF3Ph}), 7.42 (d, $^3J_{H,H}$ = 8.1 Hz, 2H, *o*-CH_{pCF3Ph}), 5.21 (s, 1H, C*H*), 3.76 (s, 3H, COOCH_3), 2.01 (s, 3H, CH_3). – ^{13}C{^{1}H} NMR (100.61 MHz, $CDCl_3$, 297 K): δ = 170.7 (*C*ONH), 167.6 (*C*OOCH$_3$), 150.0 (*C*=CH), 142.8 (*C*–C$_6$H$_4$CF$_3$), 134.6 (*C*–CH$_3$), 134.1 (d, $^5J_{C,F}$=1.3 Hz, *ipso*-C_{pCF3Ph}), 131.4 (q, $^2J_{C,F}$=32.8 Hz, *C*–CF$_3$), 129.7 (s, *o*-*C*H$_{pCF3Ph}$), 125.9 (q, $^3J_{C,F}$ = 3.7 Hz, *m*-*C*H$_{pCF3Ph}$), 123.9 (q, $^1J_{C,F}$ = 272.5 Hz, *C*F$_3$), 96.5 (C=*C*H), 52.0 (COO*C*H$_3$), 9.6 (*C*H$_3$). – ^{19}F NMR (376.58 MHz, $CDCl_3$, 297 K): δ = – 62.84 (s, C*F*$_3$). – IR (ATR): 3247 (m, br), 3082 (m), 3001 (m), 2952 (m), 1687 (s), 1625 (m), 1428 (m), 1408 (m), 1380 (m), 1357 (m), 1319 (s), 1266 (m), 1173 (s), 1106 (s), 1064 (s), 1048 (s), 1014 (s), 991 (m), 957 (m), 876 (m), 862 (m), 845 (s), 765 (s), 747 (m), 733 (m), 704 (m), 694 (s), 634 (m), 612 (m), 586 (m), 535 (m), 493 (m), 437 (m), 421 (m). – MS (DEI): *m/z* (%) = 311 (100) [M]$^+$, 283 (56) [M–CO]$^+$, 280(34) [M–CH$_3$O]$^+$, 251(32) [M–CH$_3$OH–CO]$^+$, 223 (41) [M–CH$_3$OH–2CO]$^+$, 154 (18) [C$_{11}$H$_8$N]$^+$, 115 (11) [C$_9$H$_7$]$^+$. – Elemental analysis ($C_{15}H_{12}F_3NO_3$, 311.26): calcd.: C 57.88, H 3.89, N 4.50; found C 57.81, H 3.96, N 4.47.

Physical data of **5i**: Yield: 227 mg (0.60 mmol, 98%), colorless solid. – ^{1}H NMR (400.21 MHz, $CDCl_3$, 297 K): δ = 9.38 (s, 1H, N*H*), 7.99 (s, 1H, *p*-C$H_{m(CF3)2Ph}$), 7.75 (s, 2H, *o*-C$H_{m(CF3)2Ph}$), 5.14 (s, 1H, C*H*), 3.78 (s, 3H, COOCH_3), 2.02 (s, 3H, CH_3). – ^{13}C{^{1}H} NMR (100.63 MHz, $CDCl_3$, 297 K): δ = 170.1 (*C*ONH), 167.4 (*C*OOCH$_3$), 149.5 (*C*=CH), 141.1 (*C*–C$_6$H$_3$(CF$_3$)$_2$), 136.0 (*C*–CH$_3$), 132.7 (*ipso*-$C_{m(CF3)2Ph}$), 132.7 (q, $^2J_{C,F}$ = 33.9 Hz, *C*–CF$_3$), 129.4 (d, $^3J_{C,F}$ = 3.1 Hz, *o*-*C*H$_{m(CF3)2Ph}$), 123.2 (q, $^3J_{C,F}$ = 3.8 Hz, *p*-*C*H$_{m(CF3)2Ph}$), 123.0 (q, $^1J_{C,F}$ = 272.8 Hz, *C*F$_3$), 96.5 (C=*C*H), 52.1 (COO*C*H$_3$), 9.7 (*C*H$_3$). – ^{19}**F** NMR (376.58 MHz, $CDCl_3$, 297 K): δ = – 62.90 (s, C*F*$_3$). – IR (ATR): 3404 (m), 3060 (w), 2957 (w), 1720 (s), 1691 (s), 1665 (m), 1638 (s), 1444 (m), 1411 (m), 1396 (m), 1380 (m), 1321 (m), 1281 (s), 1261 (s), 1206 (m), 1176 (s), 1158 (s), 1111 (s), 1049 (m), 1033 (m), 1000 (m), 955 (m), 934 (m), 913 (s), 873 (m), 848 (m), 831 (s), 759 (m), 712 (m), 681 (s), 650 (m), 627 (m), 600 (s), 493 (m), 447 (m), 417 (m). – MS (DEI): *m/z* (%) = 379 (100) [M]$^+$, 351 (47) [M–CO]$^+$, 348 (99) [M–CH$_3$O]$^+$, 319 (23) [M–CH$_3$OH–CO]$^+$, 291 (36) [M–CH$_3$OH–2CO]$^+$. – Elemental analysis ($C_{16}H_{11}F_6NO_3$, 379.26): calcd.: C 50.67, H 2.92, N 3.69; found C 50.54, H 3.06, N 3.38.

4.3 General procedure for 3-(4-(trifluoromethyl)phenyl)- and 3-(3,5-bis(trifluoromethyl)phenyl)-substituted methyl (*Z*)-2-(4-methyl-5-oxo-1,5-dihydro-2*H*-pyrrol-2-ylidene) acetic acids (6h and 6i)

Solutions of the methyl esters **5h** and **5k** in THF (3.9–4.7 mL mmol^{-1}) were reacted with 3 equiv. of an aqueous 2 M LiOH solution at 0°C and then at r. t. for additional 25–27 h. Diluted hydrochloric acid was added till a pH value of 2 was realized. Then 20 mL of ethyl acetate was added and

the remaining aqueous phase extracted three times with 10 mL of ethyl acetate. The combined organic phases were washed with 10 mL of a saturated NaCl solution and dried over anhydrous Na_2SO_4. After filtration, the solvent of the filtrate was removed *in vacuo*. Purity was checked by NMR spectroscopy and the acids **6h** and **6i** were used for transformations without further purification.

Physical data of **6h**: Yield: 175 mg (0.59 mmol, 92%). – ^{1}H NMR (400.13 MHz, DMSO-d_6, 296 K): δ = 12.68 (s, br, 1H, COO*H*), 10.04 (s, 1H, N*H*), 7.89 (d, $^3J_{H,H}$ = 8.1 Hz, 2H, *m*-CH_{pCF3Ph}), 7.62 (d, $^3J_{H,H}$ = 8.0 Hz, 2H, *o*-CH_{pCF3Ph}), 5.03 (s, 1H, C*H*), 1.88 (s, 3H, CH_3). – ^{13}C{^{1}H} NMR (100.61 MHz, DMSO-d_6, 296 K): δ = 170.5 (*C*ONH), 167.2 (*C*OOH), 148.9 (*C*=CH), 142.3 (*C*–$C_6H_4CF_3$), 134.5 (d, $^5J_{C,F}$ = 1.4 Hz, *ipso*-C_{pCF3Ph}), 133.5 (*C*–CH_3), 130.2 (s, *o*-CH_{pCF3Ph}), 129.3 (q, $^2J_{C,F}$ = 32.0 Hz, *C*–CF_3), 125.7 (q, $^3J_{C,F}$ = 3.7 Hz, *m*-CH_{pCF3Ph}), 124.1 (q, $^1J_{C,F}$ = 272.3 Hz, *C*F_3), 97.4 (*C*=C*H*), 9.2 (*C*H_3). – ^{19}F NMR (376.58 MHz, DMSO-d_6, 297 K): δ = – 61.21 (s, CF_3). – IR (ATR): 3416 (w), 3268 (w), 3219–2231 (m, br), 2929 (m), 1726 (m), 1707 (m), 1676 (m), 1643 (m), 1618 (m), 1450 (m), 1409 (m), 1382 (w), 1356 (m), 1322 (s), 1296 (m), 1253 (m), 1229 (m), 1206 (m), 1167 (m), 1110 (s), 1067 (m), 1018 (m), 995 (m), 948 (m), 842 (m), 776 (m), 761 (m), 743 (m), 695 (m), 670 (m), 635 (m), 617 (m), 578 (m), 535 (m), 491 (m), 458 (m), 441 (m). – MS (DEI): *m/z* (%) = 297 (100) $[M]^+$, 280 (11) $[M–OH]^+$, 269 (36) $[M–CO]^+$, 251 (22) $[M–H_2O–CO]^+$, 225 (60) $[M+H–COOH–CO]^+$, 154 (28) $[C_{11}H_8N]^+$, 115 (21) $[C_9H_7]^+$. – Elemental analysis ($C_{14}H_{10}F_3NO_3$, 297.23): calcd.: C 56.57, H 3.39, N 4.71; found C 56.68, H 3.83, N 4.27.

Physical data of **6i**: Yield: 192 mg (0.53 mmol, 99%), pale yellow solid. – ^{1}H NMR (400.21 MHz, DMSO-d_6, 297 K): δ = 12.70 (s, br, 1H, COO*H*), 10.10 (s, 1H, N*H*), 8.24 (s, 1H, *p*-C$H_{m(CF3)2Ph}$), 8.12 (s, 2H, *o*-C$H_{m(CF3)2Ph}$), 4.97 (s, 1H, C*H*), 1.87 (s, 3H, CH_3). – ^{13}C{^{1}H} NMR (100.63 MHz, DMSO-d_6, 297 K): δ = 170.2 (*C*ONH), 167.1 (*C*OOH), 148.7 (*C*=CH), 140.9 (*C*–$C_6H_3(CF_3)_2$), 134.7 (*C*–CH_3), 133.0 (*ipso*-$C_{m(CF3)2Ph}$), 130.8 (q, $^2J_{C,F}$ = 33.2 Hz, *C*–CF_3), 130.2 (d, $^3J_{C,F}$ = 3.1 Hz, *o*-C$H_{m(CF3)2Ph}$), 123.1 (q, $^1J_{C,F}$ = 273.1 Hz, *C*F_3), 122.8 (q, $^3J_{C,F}$ = 3.6 Hz, *p*-C$H_{m(CF3)2Ph}$), 97.5 (*C*=C*H*), 9.2 (*C*H_3). – ^{19}F NMR (376.58 MHz, DMSO-d_6, 297 K): δ = –61.20 (s, CF_3). – IR (ATR): 3271 (w), 3215–2285 (w, br), 2927 (w), 1706 (m), 1679 (m), 1651 (m), 1468 (m), 1439 (m), 1404 (m), 1379 (m), 1322 (m), 1276 (s), 1213 (m), 1167 (s), 1124 (s), 1032 (m), 903 (m), 885 (m), 847 (m), 832 (m), 760 (m), 706 (m), 681 (s), 644 (m), 628 (m), 576 (m), 509 (m), 443 (m), 417 (m). – MS (DEI): *m/z* (%) = 365 (100) $[M]^+$, 348 (22) $[M–OH]^+$, 337 (29) $[M–CO]^+$, 319 (22) $[M–H_2O–CO]^+$, 293 (72) $[M+H–COOH–CO]^+$. – Elemental analysis ($C_{15}H_9F_6NO_3$, 365.23): calcd.: C 49.33, H 2.48, N 3.84; found C 49.83, H 3.07, N 3.38.

4.4 General procedure for 3-(4-trifluoromethylphenyl)- and 3-(3,5-bis(trifluoromethyl)phenyl)-substituted methyl (*Z*)-2-(4-methyl-5-oxo-1,5-dihydro-2*H*-pyrrol-2-ylidene) acetyl chlorides (7h and 7i)

A drop of DMF and 1.3 equivalents of DCM were added at r. t. to a solution of the acetic acids **6h** and **6i**. After stirring for 2 h and ceased gas evolution the volatiles were removed *in vacuo*. The remaining solid was dried *in vacuo* and these products **7h** and **7i** were used for the final conversion without further purification.

Physical data of **7h**: Yield: 170 mg (0.54 mmol, 95%), light brown solid. – ^{1}H NMR (400.13 MHz, [D_8]THF, 297 K): δ = 10.24 (s, br, 1H, N*H*), 7.85 (d, $^3J_{H,H}$ = 8.2 Hz, 2H, *m*-CH_{pCF3Ph}), 7.58 (d, $^3J_{H,H}$ = 8.1 Hz, 2H, *o*-CH_{pCF3Ph}), 5.40 (s, 1H, C*H*), 1.95 (s, 3H, CH_3). – ^{13}C{^{1}H} NMR (100.61 MHz, [D_8]THF, 297 K): δ = 171.8 (*C*ONH), 164.4 (*C*OCl), 153.8 (*C*=CH), 143.8 (*C*–$C_6H_4CF_3$), 136.8 (*C*–CH_3), 135.0 (*ipso*-C_{pCF3Ph}), 131.9 (q, $^2J_{C,F}$ = 32.4 Hz, *C*–CF_3), 130.9 (s, *o*-CH_{pCF3Ph}), 126.7 (q, $^3J_{C,F}$ = 3.8 Hz, *m*-CH_{pCF3Ph}), 125.1 (q, $^1J_{C,F}$ = 272.2 Hz, *C*F_3), 100.4 (*C*=C*H*), 9.4 (*C*H_3). – ^{19}F NMR (376.58 MHz, [D_8]THF, 297 K): δ = – 63.60 (s, CF_3). – MS (DEI): *m/z* (%) = 315 (41) $[M]^+$, 280 (100) $[M–Cl]^+$.– HRMS (EI): *m/z* = 315.0279 (calcd. 315.0274 for $C_{14}H_9ClF_3NO_2$, $[M]^+$.

Physical data for **7i**: Yield: 160 mg (0.42 mmol, 99%), brown solid. – ^{1}H NMR (400.13 MHz, [D_8]THF, 297 K): δ = 10.34 (s, br, 1H, N*H*), 8.19 (s, 1H, *p*-C$H_{m(CF3)2Ph}$), 8.02 (s, 2H, *o*-C$H_{m(CF3)2Ph}$), 5.37 (s, 1H, C*H*), 1.94 (s, 3H, CH_3). – ^{13}C{^{1}H} NMR (100.61 MHz, [D_8]THF, 297 K): δ = 171.5 (*C*ONH), 164.4 (*C*OCl), 153.4 (*C*=CH), 142.5 (*C*–$C_6H_3(CF_3)_2$), 138.0 (*C*–CH_3), 133.7 (*ipso*-$C_{m(CF3)2Ph}$), 133.0 (q, $^2J_{C,F}$ = 33.5 Hz, *C*–CF_3), 130.8 (q, $^3J_{C,F}$ = 3.9 Hz, *o*-C$H_{m(CF3)2Ph}$), 124.3 (q, $^1J_{C,F}$ = 272.7 Hz, *C*F_3), 124.1 (q, $^3J_{C,F}$ = 3.6 Hz, *p*-C$H_{m(CF3)2Ph}$), 100.6 (*C*=C*H*), 9.4 (*C*H_3). – ^{19}F NMR (376.58 MHz, [D_8]THF, 297 K): δ = – 65.52 (s, CF_3). – MS (DEI): *m/z* (%) = 383 (19) $[M]^+$, 348 (100) $[M–Cl]^+$.

4.5 General procedure for 3-(4-trifluoromethylphenyl)- and 3-(3,5-bis(trifluoromethyl)phenyl)-substituted methyl (*Z*)-2-(4-methyl-5-oxo-1,5-dihydro-2*H*-pyrrol-2-ylidene) acetamides (8h and 8i)

Ammonia was passed into a solution of the acetyl chlorides **7h** and **7i** in anhydrous THF at 0°C. After 30 min the cooling bath was removed and ammonia was passed into this reaction mixture for approximately an additional

hour. During this time the clouding of the solution intensified. Thereafter the solvent was removed *in vacuo* and the residue was purified as given below.

Purification and physical data for **8h**: The residue was washed four times with 3 mL of water and dried *in vacuo*. Recrystallization from methanol yielded yellow crystals of **8h** · 0.55MeOH. Yield: 106 mg (0.34 mmol, 67%). Methanol-free samples were obtained by dissolution of **8h** · 0.55MeOH in acetone and distillation to remove MeOH. The residue was suspended in diethyl ether and the solvent removed *in vacuo*. Thereafter, the colorless residue was thoroughly dried *in vacuo*. – ^{1}H NMR (400.13 MHz, DMSO-d_6, 297 K): δ = 10.09 (s, 1H, N*H*), 7.91 (d, $^3J_{H,H}$ = 8.1 Hz, 2H, *m*-C$H_{p\text{CF3Ph}}$), 7.68 (s, 1H, NH_2), 7.63 (d, $^3J_{H,H}$ = 8.0 Hz, 2H, *o*-C$H_{p\text{CF3Ph}}$), 7.27 (s, 1H, NH_2), 5.36 (s, 1H, C*H*), 1.88 (s, 3H, CH_3). – ^{13}C{^{1}H} NMR (100.61 MHz, DMSO-d_6, 297 K): δ = 170.0 (*C*ONH), 167.7 (*C*ONH$_2$), 146.0 (*C*=CH), 142.1 (*C*–C$_6$H$_4$CF$_3$), 134.9 (d, $^5J_{C,F}$ = 1.2 Hz, *ipso*-$C_{p\text{CF3Ph}}$), 132.7 (*C*–CH$_3$), 130,2 (s, *o*-C$H_{p\text{-CF3Ph}}$), 129.2 (q, $^2J_{C,F}$ = 31.9 Hz, *C*–CF$_3$), 125.7 (q, $^3J_{C,F}$ = 3.7 Hz, *m*-C$H_{p\text{CF3Ph}}$), 124.1 (q, $^1J_{C,F}$ = 272.3 Hz, *C*F$_3$), 100.3 (*C*=*C*H), 9.1 (*C*H$_3$). – ^{19}F NMR (376.58 MHz, DMSO-d_6, 297 K): δ = –61.21 (s, C*F*$_3$). – IR (ATR): 3359 (m), 3151 (m), 2920 (w), 2790 (w), 1703 (s), 1665 (s), 1649 (s), 1609 (s), 1434 (m), 1410 (m), 1388 (m), 1360 (m), 1321 (s), 1299 (s), 1262 (m), 1175 (s), 1137 (s), 1112 (s), 1066 (s), 1042 (m), 1021 (m), 997 (m), 959 (m), 933 (m), 854 (m), 838 (s), 760 (m), 743 (m), 722 (m), 706 (m), 695 (m), 647 (s), 609 (s), 586 (s), 533 (m), 491 (m), 444 (m), 419 (m). – MS (DEI): *m/z* (%) = 296 (100) [M]$^+$, 280 (23) [M–NH$_2$]$^+$, 268 (22) [M–CO]$^+$, 251 (58) [M–NH$_3$–CO]$^+$, 225 (94) [M+H–CONH$_2$–CO]$^+$, 154 (18) [C$_{11}$H$_8$N]$^+$, 115 (21) [C$_9$H$_7$]$^+$. – Elemental analysis (C$_{14}$H$_{11}$F$_3$N$_2$O$_2$, 296.25): calcd.: C 56.76, H 3.74, N 9.46; found C 56.31, H 3.94, N 9.13.

Purification and physical data for **8i**: The product was washed with water (4 × 3 mL) and dried *in vacuo*. The solid residue was dissolved in methanol and at 4°C an amorphous solid precipitated, which was collected, washed with a few milliliters of methanol and dried *in vacuo*. Yield: 68 mg (0.19 mmol, 53%), colorless solid. Single crystals were obtained by evaporation of the solvent from the methanol mother liquor. – ^{1}H NMR (400.13 MHz, DMSO-d_6, 297 K): δ = 10.14 (s, 1H, N*H*), 8.27 (s, 1H, *p*-C$H_{m(\text{CF3})2\text{Ph}}$), 8.12 (s, 2H, *o*-C$H_{m(\text{CF3})2\text{Ph}}$), 7.69 (s, 1H, N$H_2$), 7.28 (s, 1H, N$H_2$), 5.25 (s, 1H, C*H*), 1.86 (s, 3H, CH_3). – ^{13}C{^{1}H} NMR (100.63 MHz, DMSO-d_6, 297 K): δ = 169.7 (*C*ONH), 167.6 (*C*ONH$_2$), 146.0 (*C*=CH), 140.7 (*C*–C$_6$H$_3$(CF$_3$)$_2$), 134.0 (*C*–CH$_3$), 133.4 (*ipso*-$C_{m(\text{CF3})2\text{Ph}}$), 130.8 (q, $^2J_{C,F}$ = 33.2 Hz, *C*–CF$_3$), 130.2 (d, $^3J_{C,F}$ = 2.5 Hz, *o*-C$H_{m(\text{CF3})2\text{Ph}}$), 123.1 (q, $^1J_{C,F}$ = 273.0 Hz, *C*F$_3$), 122.8 (q, $^3J_{C,F}$ = 3.8 Hz, *p*-C$H_{m(\text{CF3})2\text{Ph}}$), 100.2 (*C*=*C*H), 9.1 (*C*H$_3$). – ^{19}F NMR (376.58 MHz, DMSO-d_6, 297 K): δ = – 61.15 (s, C*F*$_3$). – IR (ATR): 3500 (m), 3417 (m), 3311 (w), 3257 (w), 3168 (m), 3066 (m), 1722 (m), 1679 (m), 1638 (m), 1600 (m), 1470 (m), 1437 (m), 1406 (m), 1376 (m), 1353 (m), 1322 (m), 1280 (s), 1238 (m), 1170 (s), 1122 (s), 1030 (m), 917 (m), 870 (m), 848 (m), 827 (m), 779 (m), 763 (m), 712 (m), 706 (m), 680 (m), 666 (m), 630 (m), 616 (m), 593 (s), 533 (m), 508 (m), 479 (s), 441 (m), 419 (m). – MS (DEI): *m/z* (%) = 364 (88) [M]$^+$, 348 (83) [M–NH$_2$]$^+$, 336 (9) [M–CO]$^+$, 319 (83) [M–NH$_3$–CO]$^+$, 293 (100) [M+H–CONH$_2$–CO]$^+$. – Elemental analysis (C$_{15}$H$_{10}$F$_6$N$_2$O$_2$, 364.25): calcd.: C 49.46, H 2.77, N 7.69; found C 49.79, H 3.43, N 7.33.

4.6 X-ray structure determinations

The intensity data for the compounds was collected on a Nonius KappaCCD diffractometer using graphite-monochromatized Mo*K*α radiation. Data was corrected for Lorentz and polarization effects; absorption was taken into account on a semi-empirical basis using multiple-scans [27–29]. The structures were solved by direct methods (SHELXS) [30] and refined by full-matrix least squares techniques against F_o^2 (SHELXL-97) [31]. The hydrogen atoms bonded to the amine groups N1A–N1D of **5f** and all other hydrogen atoms (with exception of the methyl groups C33A and C41B of **5c**) were located by difference Fourier synthesis and refined isotropically. The remaining hydrogen atoms of **5f** were included at calculated positions with fixed thermal parameters. All non-hydrogen atoms were refined anisotropically [31]. Crystallographic data as well as structure solution and refinement details are summarized in Table S2 (see Supporting Information). XP [32] and POV-RAY [33] were used for structure representations.

Crystallographic data (excluding structure factors) has been deposited with the Cambridge Crystallographic Data Centre as supplementary publication CCDC 1945677 for **2**, CCDC 1945678 for **5b**, CCDC 1945679 for **5c**, CCDC 1945680 for **5d**, CCDC 1945681 for **5e**, CCDC 1945682 for **5f**, CCDC 1945683 for **5g**, CCDC 1945684 for **5h**, CCDC 1945685 for **5j**, CCDC 1945686 for **8h**, and CCDC 1945687 for **8i**. These data can be obtained free of charge from The Cambridge Crystallographic Data Centre *via* www.ccdc.cam.ac.uk/data_request/cif.

5 Supporting information

Preparative details and characterization of 3-alkenyl- and 3-aryl-substituted methyl (*Z*)-2-(4-methyl-5-oxo-1,5-dihydro-2*H*-pyrrol-2-ylidene)acetates, crystal data and refinement details of the X-ray structure determinations, and

additional representations of the molecular structures are given as Supplementary Material available online (DOI: 10.1515/znb-2019-0125).

Acknowledgment: This work was financially supported by the Researcher Group FOR 1738 (German Research Foundation, DFG, Bonn/Germany); for more details see also the homepage at http://www.hhdp.uni-jena.de. D. S. is grateful to the Graduate Academy of the Friedrich Schiller University Jena for a finalization stipend for the dissertation. We also acknowledge the valuable support of the NMR service platform (www.nmr.uni-jena.de) and of the mass spectrometry platform (www.ms.uni-jena.de) of the Faculty of Chemistry and Earth Sciences of the Friedrich Schiller University Jena, Germany.

References

[1] D. A. Lightner, G. B. Quistad, *FEBS Lett.* **1972**, *25*, 94–96.
[2] R. Bonnett, J. C. M. Stewart, *J. Chem. Soc. Chem. Commun.* **1972**, 596–597.
[3] R. Bonnett, J. C. M. Stewart, *J. Chem. Soc. Perkin Trans. I* **1975**, 224–231.
[4] W. H. Schaefer, T. M. Harris, F. P. Guengerich, *Biochemistry* **1985**, *24*, 3254–3263.
[5] M. Ritter, R. A. Seidel, P. Bellstedt, B. Schneider, M. Bauer, H. Görls, G. Pohnert, *Org. Lett.* **2016**, *18*, 4432–4435.
[6] R. A. Seidel, M. Kahnes, M. Bauer, G. Pohnert, *J. Chromatogr. B* **2015**, *974*, 83–89.
[7] R. A. Seidel, T. Claudel, F. A. Schleser, N. K. Ojha, M. Westerhausen, S. Nietzsche, C. Sponholz, F. Cuperus, S. M. Coldewey, S. H. Heinemann, G. Pohnert, M. Trauner, M. Bauer, *J. Hepatol.* **2017**, *67*, 272–281.
[8] R. L. Macdonald, R. M. Pluta, J. H. Zhang, *Nat. Clin. Pract. Neurol.* **2007**, *3*, 256–263.
[9] K. R. Kranc, G. J. Pyne, L. Tao, T. D. W. Claridge, D. A. Harris, T. A. D. Cadoux-Hudson, J. J. Turnbull, C. J. Schofield, J. F. Clark, *Eur. J. Biochem.* **2000**, *267*, 7094–7101.
[10] M. Ritter, S. Neupane, R. A. Seidel, C. Steinbeck, G. Pohnert, *Org. Biomol. Chem.* **2018**, *16*, 3553–3555.
[11] M. Klopfleisch, R. A. Seidel, H. Görls, H. Richter, R. Beckert, W. Imhof, M. Reiher, G. Pohnert, M. Westerhausen, *Org. Lett.* **2013**, *15*, 4608–4611.
[12] R. A. Seidel, B. Schowtka, M. Klopfleisch, T. Kühl, A. Weiland, A. Koch, H. Görls, D. Imhof, G. Pohnert, M. Westerhausen, *Tetrahedron Lett.* **2014**, *55*, 6526–6529.
[13] D. Schulze, J. Traber, M. Ritter, H. Görls, G. Pohnert, M. Westerhausen, *Org. Biomol. Chem.* **2019**, *17*, 6489–6496.
[14] S. Hou, R. Xu, J. F. Clark, W. L. Wurster, S. H. Heinemann, T. Hoshi, *J. Cereb. Blood Flow Metabol.* **2011**, *31*, 102–112.
[15] A. Joerk, R. A. Seidel, S. G. Walter, A. Wiegand, M. Kahnes, M. Klopfleisch, K. Kirmse, G. Pohnert, M. Westerhausen, O. W. Witte, K. Holthoff, *J. Am. Heart Assoc.* **2014**, *3*, e001220.
[16] A. Joerk, M. Ritter, N. Langguth, R. A. Seidel, D. Freitag, K.-H. Herrmann, A. Schaefgen, M. Ritter, M. Günther, C. Sommer, D. Braemer, J. Walter, C. Ewald, R. Kalff, J. R. Reichenbach, M. Westerhausen, G. Pohnert, O. W. Witte, K. Holthoff, *Circ. Res.* **2019**, *124*, e101–e114.
[17] S. Kotha, K. Lahiri, D. Kashinath, *Tetrahedron* **2002**, *58*, 9633–9695.
[18] R. Martin, S. L. Buchwald, *Acc. Chem. Res.* **2008**, *41*, 1461–1473.
[19] H. Doucet, *Eur. J. Org. Chem.* **2008**, 2013–2030.
[20] F.-S. Han, *Chem. Soc. Rev.* **2013**, *42*, 5270–5298.
[21] A. J. J. Lennox, G. C. Lloyd-Jones, *Chem. Soc. Rev.* **2014**, *43*, 412–443.
[22] J. W. B. Fyfe, A. J. B. Watson, *Synlett* **2015**, *26*, 1139–1144.
[23] C. Li, D. Chen, W. Tang, *Synlett* **2016**, *27*, 2183–2200.
[24] J. P. G. Rygus, C. M. Crudden, *J. Am. Chem. Soc.* **2017**, *139*, 18124–18137.
[25] H.-O. Kalinowski, S. Berger, S. Braun, *^{13}C-NMR-Spektroskopie*, Georg Thieme, Stuttgart, New York, **1984**, pp. 115–117.
[26] G. R. Fulmer, A. J. M. Miller, N. H. Sherdan, H. E. Gottlieb, A. Nudelman, B. M. Stoltz, J. E. Bercaw, K. I. Goldberg, *Organometallics* **2010**, *29*, 2176–2179.
[27] R. W. W. Hooft, Collect, Nonius KappaCCD Data Collection Software, Nonius BV, Delft (The Netherlands) **1998**.
[28] Z. Otwinowski, W. Minor in *Methods in Enzymology*, Vol. *276*, *Macromolecular Crystallography, Part A* (Eds.: C. W. Carter, R. M. Sweet), Academic Press, New York, **1997**, pp. 307–326.
[29] Sadabs (version 2.10), Bruker AXS Inc., Madison, WI (USA) **2002**.
[30] G. M. Sheldrick, *Acta Crystallogr.* **2008**, *A64*, 112–122.
[31] G. M. Sheldrick, *Acta Crystallogr.* **2015**, *C71*, 3–8.
[32] XP, Siemens Analytical X-Ray Instruments Inc., Karlsruhe (Germany) **1990**; Madison, WI (USA) **1994**.
[33] POV-Ray, Trademark of Persistence of Vision Raytracer Pty. Ltd., Williamstown, Victoria (Australia); Copyright Hallam Oaks Pty. Ltd., **2007**.

Supplementary Material: The online version of this article offers supplementary material (https://doi.org/10.1515/znb-2019-0125).